The Journal of the Acoustical Society of America

SEPTEMBER 17 2020

Coherence-based performance analysis on noise reduction in multichannel active noise control systems

Jihui Aimee Zhang ; Naoki Murata; Yu Maeno; Prasanga N. Samarasinghe ; Thushara D. Abhayapala; Yuki Mitsufuji

J. Acoust. Soc. Am. 148, 1519–1528 (2020)
https://doi.org/10.1121/10.0001938

JASA ARTICLE

Coherence-based performance analysis on noise reduction in multichannel active noise control systems

Jihui Aimee Zhang,[1,a)] Naoki Murata,[2,b)] Yu Maeno,[2,c)] Prasanga N. Samarasinghe,[1,d)] Thushara D. Abhayapala,[1,e)] and Yuki Mitsufuji[2,f)]

[1]*Audio and Acoustic Signal Processing Group, The Australian National University, Canberra, Australian Central Territory 2601, Australia*

[2]*R&D Center, Sony Corporation, 2-10-1 Osaki, Shinagawa, Tokyo 141-8610, Japan*

ABSTRACT:

Active noise control (ANC) over an extended spatial region using multiple microphones and multiple loudspeakers has become an important problem. The maximum noise reduction (NR) potential over the control area is a critical evaluation variable as it indicates the fundamental limitation of a given ANC system. In this paper, a method to mathematically formulate the NR potential for any given multichannel ANC systems is developed. First, the residual error in the multichannel feedforward ANC system is formulated, and then the multiple-input-multiple-output problem is decomposed into the parallel-channel problem. The total energy of the residual error is further decomposed into three different terms representing (i) the signal coherence between the reference signals and error signals, (ii) the filter, and (iii) the system null space. The experimental results validate the proposed evaluation method and illustrate the effectiveness on the maximum NR performance evaluation for given systems. Using the proposed analyzing method, more insight into the contribution of each component to the NR potential can be achieved.

 https://doi.org/10.1121/10.0001938

(Received 9 January 2020; revised 24 July 2020; accepted 24 August 2020; published online 17 September 2020)

[Editor: Julien de Rosny] Pages: 1519–1528

I. INTRODUCTION

A. Motivation and scope

Active noise control (ANC) utilises secondary sound sources to cancel primary noise based on the principle of destructive interference and has the advantage of high flexibility and easy adaptability. Multichannel ANC systems,[1,2] equipped with multiple sensors and multiple secondary sources, are applied to achieve noise cancellation over a spatially extended region. There are many aspects to evaluate the adaptive ANC performance such as maximum noise attenuation, convergence rate,[3,4] computational complexity,[5–7] and stability and robustness.[8] In this paper, we focus on the fundamental limits of the noise reduction (NR) level for a given multichannel ANC system.

Since the NR level in the steady state varies with different adaptive algorithms, it is important to investigate the fundamental limitation of the maximum achievable performance. This method should be independent of any adaptive algorithms and has the capability to analyze the maximum NR in any arbitrary ANC system.

B. Literature review

In the literature, most performance evaluation frameworks are for specific ANC systems.[9–12] There are some investigations about the performance of different multichannel adaptive ANC algorithms.[13,14] In these investigations, either the reference signals are obtained directly from the electronic signal without the actual sensors[13] or the reference signals on the reference sensors are assumed to be fully correlated with the primary signals on the error sensors,[12,14] which are not applicable in many real applications.

In some investigations, coherence has been taken into consideration. Buerger *et al.* investigated the coherence between two observation points in the noise field evoked by given continuous source distributions, which can be applied to predict the upper bound of the ANC performance.[15] Kuo and Morgan investigated the relation between the minimum residual error and the coherence between the reference microphone and the error microphone,[16] which provided the solution in the single channel ANC systems. Bitzer *et al.* found that the complex coherence function of the noise field for all sensors is a valuable tool to examine the theoretical limits of NR for speech recognition.[17] The complex coherence function is also valuable in ANC, although the authors only evaluated the complex function for speech recognition.

Overall, to the best of our knowledge, the maximum NR performance of the multichannel ANC system for any arbitrary system has not been reported in the literature, and the coherence between sensors needs to be considered in the investigation.

C. Our contributions

In this paper, we investigate the maximum NR performance for a multichannel ANC system by investigating the

[a)]Electronic mail: jihui.zhang@anu.edu.au, ORCID: 0000-0001-6817-139X.
[b)]ORCID: 0000-0001-7418-5173.
[c)]ORCID: 0000-0001-7754-0054.
[d)]ORCID: 0000-0002-5589-4203.
[e)]ORCID: 0000-0001-6937-7218.
[f)]ORCID: 0000-0002-6806-6140.

different factors that can influence the energy of the residual error. We derive the optimal filter statistically and incorporate the coherence between the reference signals and the error signals to the maximum ANC performance analysis. We mathematically formulate the limitation for the NR in any given feedforward ANC system and analyze the three different terms in the energy of the residual signals. The theory developed in this paper can also be applied to the feedback ANC system by replacing the reference signals with the synthesized reference signals. Experiments are conducted to validate the proposed formulation and illustrate the applications for different ANC systems. One example of the application is ANC in an office room when the configurations of secondary loudspeakers and microphones have constraints on both the numbers and locations as shown in Fig. 1.

The rest of the paper is organized as follows. Section II presents the problem formulation and Sec. III presents mathematical derivations of the energy of the residual error and its different components. We demonstrate the experimental results to validate the proposed method and illustrate the potential application in Sec. IV and draw some conclusions in Sec. V.

II. PROBLEM FORMULATION

Consider a multichannel feedforward ANC system with Q error microphones, P reference microphones, and L secondary sources. The residual signal at the qth error microphone is given by

$$e_q(k) = \nu_q(k) + s_q(k), \tag{1}$$

where $k = 2\pi f/c$ is the wavenumber, f is the frequency, c is the speed of sound propagation, $\nu_q(k)$ and $s_q(k)$ are the primary sound field due to noise and the secondary sound field generated by the secondary sources at the qth error microphone, respectively. We write Eq. (1) in vector form by defining a vector of error signals at Q microphones as

$$\boldsymbol{e}(k) = \boldsymbol{v}(k) + \boldsymbol{s}(k), \tag{2}$$

where $\boldsymbol{e}(k) = [e_1(k), \ldots, e_Q(k)]^T$, $\boldsymbol{v}(k) = [\nu_1(k), \ldots, \nu_Q(k)]^T$, $\boldsymbol{s}(k) = [s_1(k), \ldots, s_Q(k)]^T$, and $[\cdot]^T$ is the transpose operator.

Let $x_p(k)$, $p = 1, \ldots, P$, be the reference signal at the pth reference microphone. In feedforward ANC systems, the signals driving the secondary sources are generated by adaptive filtering of reference signals that is measured closer to the noise sources. Thus, the secondary sound field at the qth error microphone can be represented as

$$s_q(k) = \sum_{\ell=1}^{L} G_{q\ell}(k) \left(\sum_{p=1}^{P} w_{\ell p}(k) x_p(k) \right), \tag{3}$$

where $w_{\ell p}(k)$ is the adaptive filter between the pth reference microphone and the ℓth secondary source, and $G_{q\ell}(k)$ is the acoustic transfer function (ATF) from the ℓth secondary source to the qth error microphone. We rewrite Eq. (3) in vector form as

$$\boldsymbol{s}(k) = \boldsymbol{G}(k)\boldsymbol{W}(k)\boldsymbol{x}(k), \tag{4}$$

where $\boldsymbol{G}(k)$ is a $Q \times L$ matrix with the (q, ℓ) element given by $G_{q\ell}(k)$, $\boldsymbol{W}(k)$ is an $L \times P$ matrix of adaptive filters with the (ℓ, p) element given by $W_{\ell p}(k)$, and $\boldsymbol{x}(k) = [x_1(k), \ldots, x_P(k)]^T$.

We substitute Eq. (4) into Eq. (2) to express the error signal vector in terms of the adaptive filter weights of secondary sources, reference signals, and secondary signal paths as

$$\boldsymbol{e}(k) = \boldsymbol{v}(k) + \boldsymbol{G}(k)\boldsymbol{W}(k)\boldsymbol{x}(k). \tag{5}$$

In a typical adaptive ANC system, as illustrated in the block diagram of Fig. 2, the filter $\boldsymbol{W}(k)$ is updated iteratively. For the rest of this paper, we omit the dependency k of all quantities for notational convenience.

The aim of multichannel ANC systems is to minimise the residual signal at the error microphones. The total energy of Q error signals is

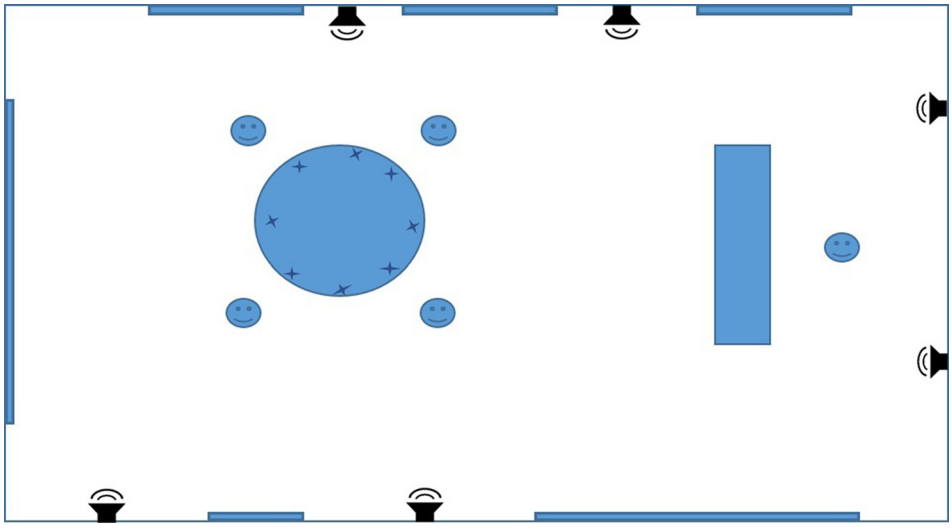

FIG. 1. (Color online) An illustration of an ANC system in an office room with a meeting table and a desk. The error microphones are placed on the table. Door, windows, and whiteboard are located in three sides of the walls. Due to the limited space, the configurations of the secondary loudspeakers and reference microphones have constraints on both the numbers and locations, and the proposed method can be used to analyze and optimize the configurations by predicting the contributions of each component.

https://doi.org/10.1121/10.0001938

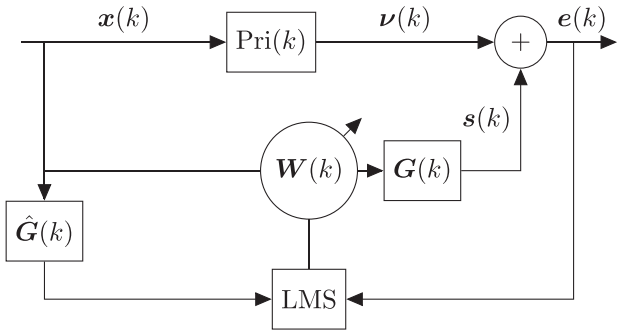

FIG. 2. Block diagram of a typical multichannel feedforward ANC system, where $\boldsymbol{x}(k)$, $\boldsymbol{v}(k)$, and $\boldsymbol{e}(k)$ denote the reference signals, primary signals, and error signals, respectively, $\boldsymbol{W}(k)$ denotes the filter, $\mathrm{Pri}(k)$ and $\boldsymbol{G}(k)$ denote the primary path and secondary path, respectively, $\hat{\boldsymbol{G}}(k)$ denotes the estimation of the secondary path, and LMS denotes the adaptive algorithm.

$$\begin{aligned}\mathcal{E}_T &= E\left\{\sum_{q=1}^{Q}|e_q|^2\right\}\\ &= E\{\boldsymbol{e}^H\boldsymbol{e}\}\\ &= E\{\boldsymbol{v}^H\boldsymbol{v}\}+E\{\boldsymbol{v}^H\boldsymbol{G}\boldsymbol{W}\boldsymbol{x}\}+E\{\boldsymbol{x}^H\boldsymbol{W}^H\boldsymbol{G}^H\boldsymbol{v}\}\\ &\quad+E\{\boldsymbol{x}^H\boldsymbol{W}^H\boldsymbol{G}^H\boldsymbol{G}\boldsymbol{W}\boldsymbol{x}\},\end{aligned} \tag{6}$$

where $E\{\cdot\}$ denotes the mathematical expectation, $[\cdot]^H$ denotes the complex conjugate transpose of a vector or matrix, and the last line is obtained by substituting for $\boldsymbol{e}$ from Eq. (5). Note that $\mathcal{E}_T$ can be regarded as the sum of the power spectral density of Q error signals.

In this paper, we seek to analyze the residual error $\mathcal{E}_T$ given by Eq. (6). Particularly, we are interested in its dependency on the (i) coherence between reference signals at the reference microphones and primary signals at the error microphones, (ii) characteristics of the secondary channels between secondary sources and error microphones, and (iii) correlation between reference signals.

III. ANALYSIS OF RESIDUAL ERROR

In this section, we first analyze the secondary path $\boldsymbol{G}$ and the power spectral density of the reference signals $\boldsymbol{S}_{\boldsymbol{xx}}$ in the eigen-domain to further investigate the representation of the total energy of the error signals in Eq. (6) and then discuss the different components of the representation. We also illustrate a special case, which links back to the conventional single channel case as reported in the literature.[16]

A. Singular value decomposition of the secondary path

The secondary acoustic paths $G_{q\ell}$, $q = 1, \ldots, Q$, $\ell = 1, \ldots, L$, are not necessarily independent of each other. To reveal the underlying structure, we express the ATF matrix $\boldsymbol{G}$ in terms of its singular value decomposition (SVD) form as

$$\boldsymbol{G} = \boldsymbol{A}\boldsymbol{\Sigma}\boldsymbol{B}^H, \tag{7}$$

where the $Q \times Q$ matrix $\boldsymbol{A}$ contains the left-singular vectors, the $L \times L$ matrix $\boldsymbol{B}$ contains the right-singular vectors, and the $Q \times L$ rectangular diagonal matrix $\boldsymbol{\Sigma}$ contains the singular values. Let the nonzero diagonal entries of $\boldsymbol{\Sigma}$, denoted by σ_r, $r = 1, \ldots, R$, where $R = \mathrm{rank}(\boldsymbol{G}) \leqslant \min\{Q, L\}$ is the number of nonzero diagonal elements of $\boldsymbol{\Sigma}$.

Let $a_{qq'}$ be the (q, q') element of $\boldsymbol{A}$ and $b_{\ell\ell'}$ be the (ℓ, ℓ') element of $\boldsymbol{B}$. For convenience, we write $\boldsymbol{A} = [\boldsymbol{a}_1, \boldsymbol{a}_2, \ldots, \boldsymbol{a}_Q]$ and $\boldsymbol{B} = [\boldsymbol{b}_1, \boldsymbol{b}_2, \ldots, \boldsymbol{b}_L]$, where $\boldsymbol{a}_q = [a_{1q}, \ldots, a_{Qq}]^T$ and $\boldsymbol{b}_\ell = [b_{1\ell}, \ldots, b_{L\ell}]^T$ are the qth left and ℓ th right singular vectors, respectively. Also note that by the definition of SVD, $\boldsymbol{A}\boldsymbol{A}^H = \boldsymbol{I}_Q$ and $\boldsymbol{B}\boldsymbol{B}^H = \boldsymbol{I}_L$, where $\boldsymbol{I}_Q$ and $\boldsymbol{I}_L$ are identity matrices with dimensions $Q \times Q$ and $L \times L$, respectively.

B. Eigen analysis of the reference signals

For each frequency bin, the reference signals x_p, $p = 1 \ldots, P$, could be correlated with each other due to the placement of the reference microphones, the acoustic environment, and any dependency between noise sources. The power spectral density matrix of the reference signals $\boldsymbol{S}_{\boldsymbol{xx}} \triangleq E\{\boldsymbol{x}\boldsymbol{x}^H\}$ is generally ill-conditioned due to the linear relations between the channels.[18] To gain insights, we analyze the power spectral density matrix of the reference signals $\boldsymbol{S}_{\boldsymbol{xx}}$ using the eigendecomposition as

$$\boldsymbol{S}_{\boldsymbol{xx}} = \boldsymbol{U}\boldsymbol{\Lambda}\boldsymbol{U}^{-1}, \tag{8}$$

where $\boldsymbol{U}$ is the $P \times P$ eigenvector matrix and $\boldsymbol{\Lambda}$ is a $P \times P$ diagonal matrix of eigenvalues. We denote λ_z as the zth nonzero eigenvalue, $z = 1, \ldots, Z$, where $Z \leqslant P$ is the number of nonzero eigenvalues.

Let $u_{pp'}$ be the (p, p') element of $\boldsymbol{U}$, then $\boldsymbol{U} = [\boldsymbol{u}_1, \boldsymbol{u}_2, \ldots, \boldsymbol{u}_P]$ with the pth eigenvector given by $\boldsymbol{u}_p = [u_{1p}, \ldots, u_{Pp}]^T$. Here, the vectors $\boldsymbol{u}_1, \boldsymbol{u}_2, \ldots, \boldsymbol{u}_P$ are written in order of descending eigenvalues in $\boldsymbol{\Lambda}$.

Since $\boldsymbol{S}_{\boldsymbol{xx}}$ is a Hermitian matrix, all eigenvalues of $\boldsymbol{\Lambda}$ are real. Based on the spectral theorem, there exists an orthonormal basis $\boldsymbol{U}$, consisting of eigenvectors of the Hermitian matrix $\boldsymbol{S}_{\boldsymbol{xx}}$, i.e., $\boldsymbol{U}^{-1} = \boldsymbol{U}^H$, where $(\cdot)^{-1}$ denotes the matrix inverse. Then, Eq. (8) can be rewritten as

$$\boldsymbol{S}_{\boldsymbol{xx}} = \boldsymbol{U}\boldsymbol{\Lambda}\boldsymbol{U}^H. \tag{9}$$

Using the eigenvectors corresponding to Z nonzero eigenvalues, we can construct a vector space that spans all reference signals $\boldsymbol{x}$ for a given environment. Thus, we express the reference signal $\boldsymbol{x}$ in terms of these eigenvectors as

$$\boldsymbol{x} = \sum_{z=1}^{Z} c_z\boldsymbol{u}_z \tag{10}$$

$$= \hat{\boldsymbol{U}}\boldsymbol{c}, \tag{11}$$

where $\hat{\boldsymbol{U}} = [\boldsymbol{u}_1, \ldots, \boldsymbol{u}_Z]$, $\boldsymbol{c} = [c_1, \ldots, c_Z]^T$ is a vector of coefficients of reference signal $\boldsymbol{x}$, and each coefficient

$$c_z = \boldsymbol{u}_z^H\boldsymbol{x}. \tag{12}$$

The vector form can be represented as

$$\boldsymbol{c} = \hat{\boldsymbol{U}}^H \boldsymbol{x}. \tag{13}$$

Consider the correlation between c_z

$$E\{\boldsymbol{c}\boldsymbol{c}^H\} = E\{\hat{\boldsymbol{U}}^H \boldsymbol{x}(\hat{\boldsymbol{U}}^H \boldsymbol{x})^H\} = \hat{\boldsymbol{U}}^H \boldsymbol{S}_{\boldsymbol{xx}} \hat{\boldsymbol{U}} = \boldsymbol{\Lambda}. \tag{14}$$

Thus, for $z \leq Z$,

$$E\{c_z^* c_{z'}\} = \begin{cases} \lambda_z, & z = z', \\ 0, & z \neq z', \end{cases} \tag{15}$$

where $\lambda_z \neq 0$, and $[\cdot]^*$ denotes the complex conjugate of a vector or matrix. Therefore, the components of $\boldsymbol{c}$ are mutually orthogonal. Thus, using Eq. (13), we have transformed (possibly) correlated P reference signals $\boldsymbol{x}$ to $Z(\leq P)$ uncorrelated signals $\boldsymbol{c}$.

By the SVD of the secondary path (Sec. III A) and the eigendecomposition of the reference signals (Sec. III B), we decompose the multiple-input-multiple-output processing [Fig. 3(a)] into parallel-channel processing [Fig. 3(b)]. Thereafter, we represent the total energy of the error signals in the new transformed domain.

C. Representation of total energy of the error signals

For a given ANC system comprised of reference microphones, error microphones, and secondary sources in a given room environment with a particular set of noise sources, $\boldsymbol{A}$, $\boldsymbol{\Sigma}$, $\boldsymbol{B}$, $\boldsymbol{\Lambda}$, and $\boldsymbol{U}$, can be estimated using the secondary acoustic path matrix $\boldsymbol{G}$ and the measured correlation matrix of the reference signal $\boldsymbol{S}_{\boldsymbol{xx}}$.

We substitute Eqs. (7) and (11) into Eq. (6) to obtain the total energy of the error signal as

$$\begin{aligned} \mathcal{E}_T = {} & E\{\hat{\boldsymbol{v}}^H \hat{\boldsymbol{v}}\} + E\{\hat{\boldsymbol{v}}^H \boldsymbol{\Sigma} \hat{\boldsymbol{W}} \boldsymbol{c}\} + E\{\boldsymbol{c}^H \hat{\boldsymbol{W}}^H \boldsymbol{\Sigma}^H \hat{\boldsymbol{v}}\} \\ & + E\{\boldsymbol{c}^H \hat{\boldsymbol{W}}^H \boldsymbol{\Sigma}^H \boldsymbol{\Sigma} \hat{\boldsymbol{W}} \boldsymbol{c}\}, \end{aligned} \tag{16}$$

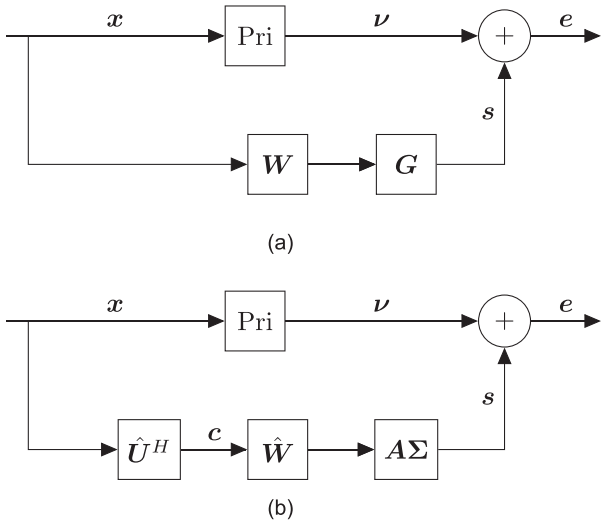

FIG. 3. Block diagram of multichannel feedforward ANC system (a) in the multichannel form and (b) decomposed into equivalent parallel channels.

where $\hat{\boldsymbol{v}} = \boldsymbol{A}^H \boldsymbol{v}$ and the $L \times Z$ matrix

$$\hat{\boldsymbol{W}} = \boldsymbol{B}^H \boldsymbol{W} \hat{\boldsymbol{U}}. \tag{17}$$

Let $\hat{\nu}_r$, $r = 1, \ldots, R$ be the rth element of $\hat{\boldsymbol{v}}$, then

$$\hat{\nu}_r = \boldsymbol{a}_r^H \boldsymbol{v}. \tag{18}$$

Also, let $\hat{w}_{\ell z}$ be the (ℓ, z) element of $\hat{\boldsymbol{W}}$, and then we define the vector $\hat{\boldsymbol{w}}_\ell \triangleq [\hat{w}_{\ell 1}, \ldots, \hat{w}_{\ell Z}]$, such that $\hat{\boldsymbol{W}} = [\hat{\boldsymbol{w}}_1, \ldots, \hat{\boldsymbol{w}}_L]^T$. We now state the main result of the paper as a theorem.

Theorem 1. *For a given ANC system, since both the correlation matrix between the error signal vector $\boldsymbol{v}$ and the reference signal vector $\boldsymbol{x}$ ($\boldsymbol{S}_{\boldsymbol{vx}} = E\{\boldsymbol{v}\boldsymbol{x}^H\}$) and the power spectral density matrix of the error signal vector $\boldsymbol{v}$ ($\boldsymbol{S}_{\boldsymbol{vv}} = E\{\boldsymbol{v}\boldsymbol{v}^H\}$) can be pre-measured, the total energy of the error signals can be represented by a sum over each eigen channel r of the secondary paths as*

$$\begin{aligned} \mathcal{E}_T = {} & \underbrace{\sum_{r=1}^{R} \left(\left(1 - \frac{\boldsymbol{S}_{\hat{\nu}_r \boldsymbol{c}} \hat{\boldsymbol{\Lambda}}^{-1} \boldsymbol{S}_{\hat{\nu}_r \boldsymbol{c}}^H}{S_{\hat{\nu}_r \hat{\nu}_r}} \right) S_{\hat{\nu}_r \hat{\nu}_r} \right)}_{\mathcal{E}_{T1}} \\ & + \underbrace{\sum_{r=1}^{R} |\sigma_r|^2 \left[\left(\hat{\boldsymbol{w}}_r + \frac{\boldsymbol{S}_{\hat{\nu}_r \boldsymbol{c}}}{\sigma_r} \hat{\boldsymbol{\Lambda}}^{-1} \right) \hat{\boldsymbol{\Lambda}} \left(\hat{\boldsymbol{w}}_r + \frac{\boldsymbol{S}_{\hat{\nu}_r \boldsymbol{c}}}{\sigma_r} \hat{\boldsymbol{\Lambda}}^{-1} \right)^H \right]}_{\mathcal{E}_{T2}} \\ & + \underbrace{\sum_{r=R+1}^{Q} S_{\hat{\nu}_r \hat{\nu}_r}}_{\mathcal{E}_{T3}}, \end{aligned} \tag{19}$$

where $\hat{\boldsymbol{\Lambda}}$ is a $Z \times Z$ diagonal matrix whose diagonal elements are the nonzero diagonal elements of $\boldsymbol{\Lambda}$, $\boldsymbol{S}_{\hat{\nu}_r \boldsymbol{c}} = E\{\hat{\nu}_r \boldsymbol{c}^H\} = \boldsymbol{a}_r^H \boldsymbol{S}_{\boldsymbol{vx}} \hat{\boldsymbol{U}}$, $S_{\hat{\nu}_r \hat{\nu}_r} = E\{\hat{\nu}_r \hat{\nu}_r^H\} = \boldsymbol{a}_r^H \boldsymbol{S}_{\boldsymbol{vv}} \boldsymbol{a}_r$, σ_r is the rth non-singular value of the secondary path matrix, R is the number of non-singular values of the secondary path matrix, and Z is the number of nonzero eigenvalues of the power spectral density matrix $\boldsymbol{S}_{\boldsymbol{xx}}$ of the reference signals.

The proof of Eq. (19) is given in Appendix A. We have the following comments on the above expression on residual error for a given frequency k.

1. Signal coherence

Observe that the first term in Eq. (19) is dependent on the correlation between various signal quantities. We can rewrite the first term as

$$\mathcal{E}_{T1} = \sum_{r=1}^{R} \left(1 - \sum_{z=1}^{Z} C_{\hat{\nu}_r c_z} \right) S_{\hat{\nu}_r \hat{\nu}_r}, \tag{20}$$

where

$$C_{\hat{\nu}_r c_z} \triangleq \frac{||S_{\hat{\nu}_r c_s}||^2}{S_{\hat{\nu}_r \hat{\nu}_r} S_{c_z c_z}} = \frac{||\boldsymbol{a}_r^H \boldsymbol{S}_{\boldsymbol{vx}} \boldsymbol{u}_z||^2}{\boldsymbol{a}_r^H \boldsymbol{S}_{\boldsymbol{vv}} \boldsymbol{a}_r \lambda_z} \tag{21}$$

https://doi.org/10.1121/10.0001938

is the coherence between the transformed primary signal $\hat{\nu}_r$ and the eigen component c_z of the reference signal.

From Eq. (20), $\mathcal{E}_{T1}$ depends on the coherence between the transformed primary signals and the transformed reference signals and the power spectral density of the transformed primary signals.

2. Filter

The second summation in Eq. (19) depends on the transformed filter $[\hat{\boldsymbol{w}}_1, \ldots, \hat{\boldsymbol{w}}_R]^T$. If we set the second part of Eq. (19), $\mathcal{E}_{T2}$, to zero, then the filter $\hat{\boldsymbol{W}}$ is optimized. The rth transformed optimal filter $\hat{\boldsymbol{w}}_r^o$ can be represented as

$$\hat{\boldsymbol{w}}_r^o = -\frac{\boldsymbol{S}_{\hat{\nu}_r \boldsymbol{e}}}{\sigma_r}\hat{\boldsymbol{\Lambda}}^{-1} = -\frac{\boldsymbol{a}_r^H \boldsymbol{S}_{\boldsymbol{vx}}\hat{\boldsymbol{U}}}{\sigma_r}\hat{\boldsymbol{\Lambda}}^{-1}. \tag{22}$$

This is equivalent to setting the differentiation of the energy of the error signal with respect to the filter $\boldsymbol{W}$ to zero. The proof is shown in Appendix B.

Observe that $\hat{\boldsymbol{w}}_r^o$ is a $1 \times Z$ vector for $r = 1, \ldots, R$, i.e., each element $\hat{w}_{rz}^o$ is the optimal weight for the corresponding eigen channel of the system. Therefore, the upper triangle elements of the transferred optimal filter in matrix form $\hat{\boldsymbol{W}}_{\text{up}}^o$ can be represented by

$$\hat{\boldsymbol{W}}_{\text{up}}^o = \begin{bmatrix} \hat{\boldsymbol{w}}_1{}^o \\ \vdots \\ \hat{\boldsymbol{w}}_R{}^o \end{bmatrix}_{R\times Z}. \tag{23}$$

Let us denote $\hat{\boldsymbol{B}} = [\boldsymbol{b}_1, \boldsymbol{b}_2, \ldots, \boldsymbol{b}_R]$ and $\hat{\boldsymbol{U}} = [\boldsymbol{u}_1, \boldsymbol{u}_2, \ldots, \boldsymbol{u}_Z]$, which correspond to the nonzero elements of $\boldsymbol{\Sigma}$ and $\boldsymbol{\Lambda}$, respectively.

From Eq. (17), the optimal filter $\boldsymbol{W}^o$ can be represented by

$$\boldsymbol{W}^o = \hat{\boldsymbol{B}}\hat{\boldsymbol{W}}_{\text{up}}^o\hat{\boldsymbol{U}}^H. \tag{24}$$

Substituting Eq. (23) into Eq. (24), we can obtain the optimal filter $\boldsymbol{W}^o$.

3. System null space

From Eq. (19), the third summation

$$\mathcal{E}_{T3} = \sum_{r=R+1}^{Q} S_{\hat{\nu}_r\hat{\nu}_r}, \tag{25}$$

where $S_{\hat{\nu}_r\hat{\nu}_r} = \boldsymbol{a}_r^H \boldsymbol{S}_{\boldsymbol{vv}}\hat{\boldsymbol{a}}_r$, $r = R+1, \ldots, Q$, i.e., $\mathcal{E}_{T3}$ is due to the components of the energy of the primary signal at the error microphones projected onto the null space of the system. This represents the noise field component, which cannot be controlled as it is in the null space. It indicates the limitation of the NR for a given system.

D. Special case: Single channel ANC system

If the system has only a single reference microphone, a single secondary source, and a single error microphone, then all the vectors and matrices in Eq. (6) are scalar valued. Thus, Eq. (6) can be rewritten as

$$\begin{aligned}\mathcal{E}_T &= E\{e^*e\} \\ &= E\{\nu^*\nu\} + E\{\nu^*gwx\} + E\{x^*w^*g^*\nu\} \\ &\quad + E\{x^*w^*g^*gwx\} \\ &= S_{\nu\nu} + gwS_{x\nu} + w^*g^*S_{\nu x} + w^*wg^*gS_{xx} \\ &= [1 - C_{\nu x}]S_{\nu\nu} + \left|gw + \frac{S_{\nu x}}{S_{xx}}\right|^2 S_{xx},\end{aligned} \tag{26}$$

where $C_{\nu x} = (|S_{\nu x}|^2)/(S_{xx}S_{\nu\nu})$ is the coherence between the primary signal ν and the reference signal x.

In Eq. (26), the first term corresponds to the signal coherence and the second term corresponds to the filter. When the filter is optimized, $w^o = -S_{\nu x}/(gS_{xx})$, the second term is equal to zero. Therefore, in a single channel ANC system, the minimum energy of the residual error only depends on the coherence of the primary signal and the reference signal. This is consistent with the finding in the literature.[16] In the single channel ANC system, Eq. (26) is also a simplified version of Eq. (19), which demonstrates that Eq. (19) is a generalized formula for the maximum NR performance in an ANC system.

IV. EXPERIMENTS

In this section, we conduct experiments in reverberant environments to validate the proposed formulation and illustrate the potential application to evaluate the ANC performance for given systems.

A. Experiment setup

1. Noise signals

We use two uncorrelated primary noises in different locations. The noise signals from each primary source are broadband noise measured from two different engines in open space. From the frequency spectrum of the noise signals, we can find that the energy of the two noise signals are both dominant in low frequency bins ([50–500] Hz) as shown in Fig. 4. Therefore, the evaluated frequency range in this validation is [100–500] Hz. In this experiment, the sampling rate is 48 kHz. We adopt a blockwise operation and transform the microphone recordings into the time-frequency domain. In the short-time Fourier transform, the frame length and the fast Fourier transform (FFT) length are 9216 samples. A Hann window with 50% overlaps is employed in the process.

2. Evaluation variables

We evaluate the ANC performance in terms of NR at the microphone locations and the contributions of different components ($\mathcal{E}_{T1}$, $\mathcal{E}_{T2}$, and $\mathcal{E}_{T3}$) in the energy of the residual signals.

The NR at the microphone locations can be represented by

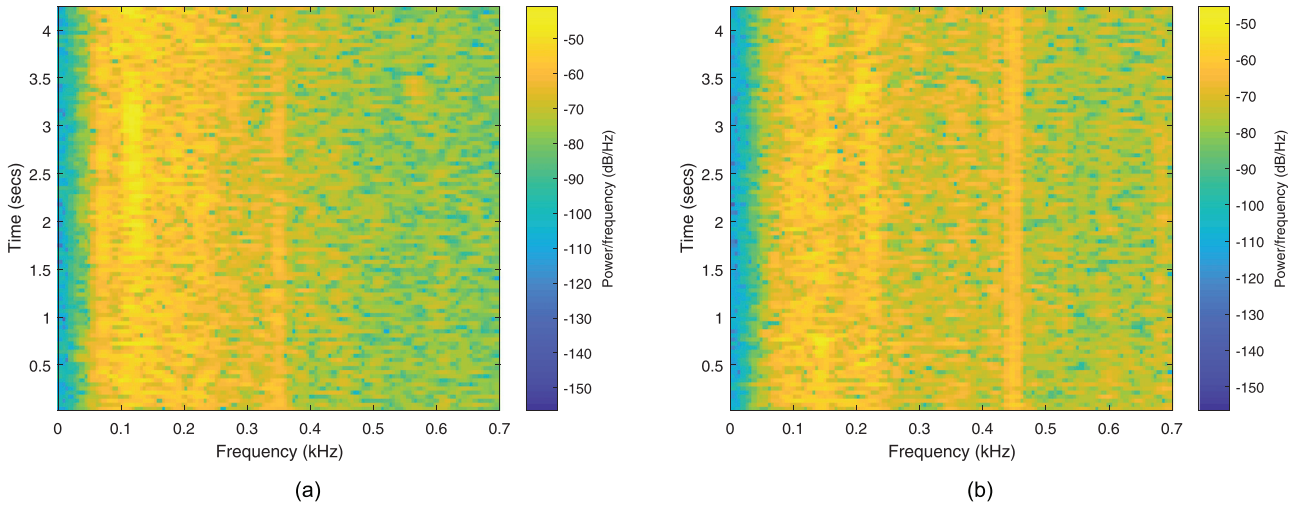

FIG. 4. (Color online) Spectrograms of the noise signals. (a) Noise signal 1 and (b) noise signal 2.

$$\mathrm{NR} = -10\log_{10}\frac{\mathcal{E}_T}{\mathcal{E}_{\mathrm{pri}}}, \tag{27}$$

where $\mathcal{E}_{\mathrm{pri}} = \Sigma_{q=1}^{Q} E\{|\nu_q|^2\}$ and $E\{|\nu_q|^2\}$ denotes the average energy of the primary noise field at the qth error microphone point.

The contribution of the jth component can be represented by

$$\mathrm{CO}_j = -10\log_{10}\frac{\mathcal{E}_{Tj}}{\mathcal{E}_{\mathrm{pri}}}, \tag{28}$$

where $\mathcal{E}_{Tj}, j = 1, 2, 3$ is each component in Eq. (19). For a given system setup, the lower the value of CO_j, the higher the corresponding contribution to the energy of residual signals.

3. ANC system setup

The experimental ANC system has been set up in the audio laboratory of the Australian National University as shown in Fig. 5. TANNOY SYSTEM 600 floorstanding speakers (Tannoy Professional) have been used as primary sources and Grover Notting CR1 speakers (Classic Audio Designs Pty Ltd.) have been used as secondary sources. We use Dyton Audio EMM-6 Electret Measurement Microphones (Dayton Audio) to measure the reference signals, primary signals, and impulse responses from the secondary sources to the error microphones. The error microphones are placed at the center of the spherical loudspeaker array (30 small loudspeakers), where 4 loudspeakers in this loudspeaker array have been chosen as the secondary sources. The reference microphones are located between the secondary sources and the primary sources.

The experiment is conducted in three different cases. In case 1, the same number (four) of reference microphones, error microphones, and secondary sources are placed in the ANC system. Compared with case 1, there are five more error microphones in case 2 and three less reference microphones in case 3. In all cases, the locations of the primary sources (two large loudspeakers) and the secondary sources (four small loudspeakers) are the same.

B. Validation of the formulation

In this section, we validate the proposed formulation using case 2. Other than using the optimal filter $\boldsymbol{W}^o$, we also evaluate the NR using the adaptive filter $\boldsymbol{W}_{\mathrm{adp}}$. The adaptive filter $\boldsymbol{W}_{\mathrm{adp}}$ is obtained through the normalized FxLMS algorithm[19] in the frequency domain. Both filter update and filtering process are conducted in the frequency domain. Blockwise adaptation has been implemented, and each iteration is based on one frame of the noise signal.

1. Maximum NR performance

We first examine the maximum NR level using the optimal filter in the proposed method $\boldsymbol{W}^o$ (red curves) and the NR level using the adaptive filter $\boldsymbol{W}_{\mathrm{adp}}$ after 48 iterations (blue curves) as shown in Fig. 6.

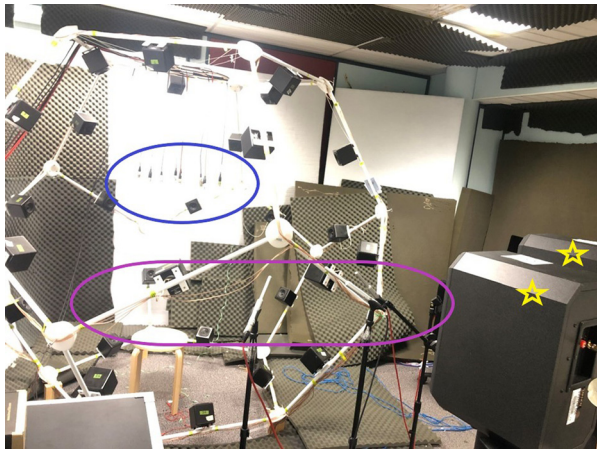

FIG. 5. (Color online) ANC system setup, in which the error microphones (blue circle) are placed at the center of the secondary source array, and the reference microphones (purple capsule) are placed between the secondary source array and the primary sources (yellow stars).

https://doi.org/10.1121/10.0001938

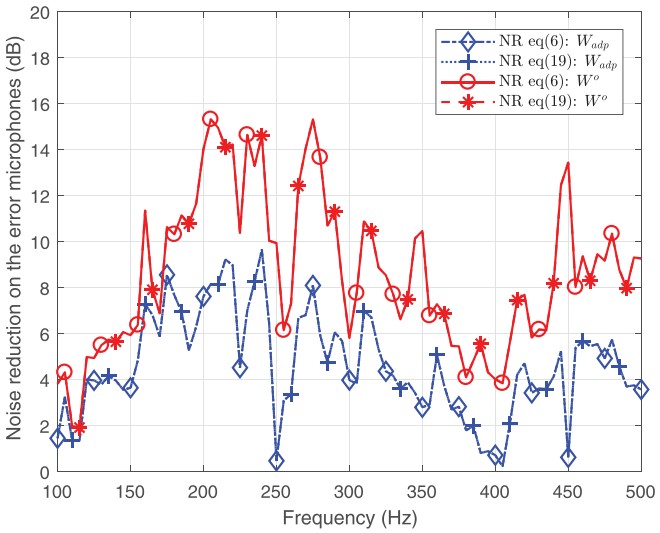

FIG. 6. (Color online) NR on the error microphones in case 2.

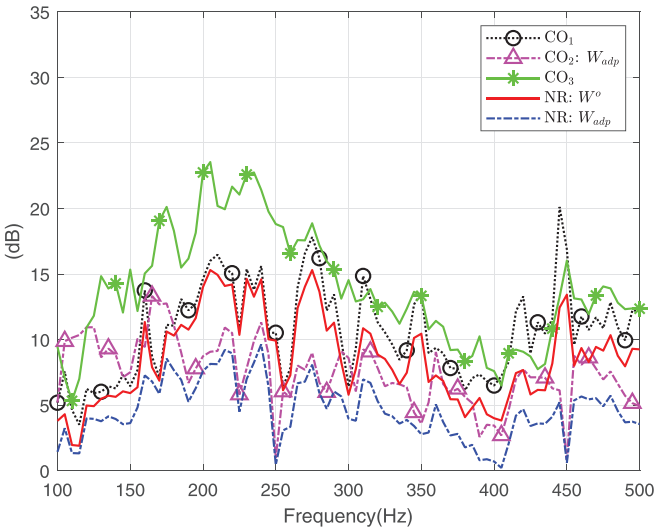

FIG. 7. (Color online) Contribution of different parts to the energy of residual signals in case 2 (dB).

In theory, the proposed analysis method [Eq. (19)] should reach the same minimum residual error as the conventional analyzing method [Eq. (6)] as long as we use the same filter $\boldsymbol{W}$. This has been confirmed in the experimental results, where two blue curves merge together and two red curves merge together.

Using the optimal filter in the proposed method ($\boldsymbol{W} = \boldsymbol{W}^o$), the NR level has comparable results to using the adaptive filter ($\boldsymbol{W} = \boldsymbol{W}_{\text{adp}}$). We also notice that the NR level derived by the proposed optimal filter (red curves) is slightly higher than the NR using the adaptive filter (blue curves), which is the same as we expected. This is due to a number of factors in the adaptive filer such as the adaptive algorithm, number of iterations, step size, stability of the noise signals, etc. Whereas maximum NR analysis using the proposed optimal filter provides a statistical estimation of the NR level for a given noise signal, ANC system, and acoustic environment.

2. Contribution of different parts in the energy of residual signals

Furthermore, we investigate the contributions of different components in the energy of the residual signals ($\mathcal{E}_T$) as shown in Fig. 7.

$\mathcal{E}_{T1}$ (black curve) depends on the coherence between the transformed reference signals and the error signals $\boldsymbol{C}_{\boldsymbol{v}'\boldsymbol{e}}$, and $\mathcal{E}_{T3}$ is due to the noise signal in the system null space. As shown in Fig. 7, $\mathcal{E}_{T1}$ has more contribution to the energy of the residual signals (red curve) compared to $\mathcal{E}_{T3}$ (green curve).

$\mathcal{E}_{T2}$ is based on the filter $\boldsymbol{W}$. For the analysis based on the proposed optimal filter, $\mathcal{E}_{T2} = 0$. For the analysis based on the adaptive filter, the contribution of $\mathcal{E}_{T2}$ exists as the filter has not been optimized yet (pink curve).

C. Potential application of this formulation

In this section, we illustrate the potential application of the proposed formulation. We use the proposed formulation to analyze the ANC system in case 1, case 2, and case 3 in the experiment.

We first compare maximum NR at the error microphones in different cases as shown in Fig. 8. In case 1, since enough secondary sources have been applied to control all the error microphones, the maximum NR level (red curve) is higher than that in case 2 (blue curve) and case 3 (black curve). In case 3, as the reference microphone number is less than the number of error microphones and the number of secondary sources, the maximum NR level is much lower than the other two cases.

Next, we compare the contributions of different parts of the minimum energy of the residual error in three different cases as shown in Fig. 9. We ignore the comparison of $\mathcal{E}_{T2}$ as $\mathcal{E}_{T2} = 0$ in all three different cases when the filters are optimized. In case 1 and case 3, rank $R = Q$. As a consequence, in both case 1 and case 3, $\mathcal{E}_{T3}$ of Eq. (19) are all zero, and $\mathcal{E}_{T1}$ is the only contribution of the minimum energy of the residual error. In case 2, as the error microphone number [Eq. (9)] is

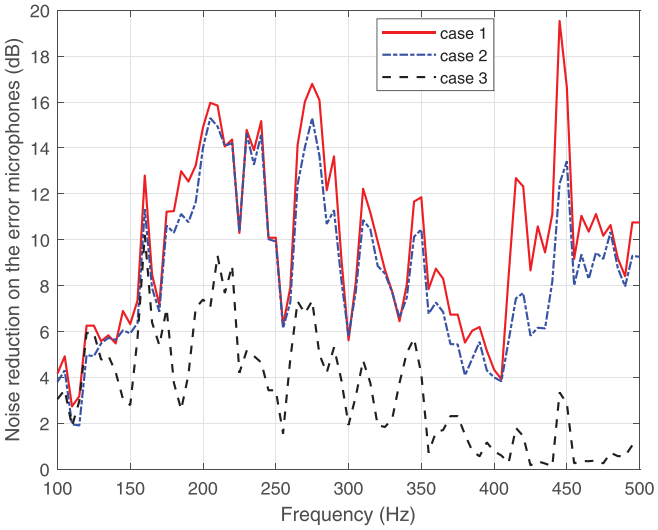

FIG. 8. (Color online) NR on the error microphones in cases 1, 2, and 3 in the experiment.

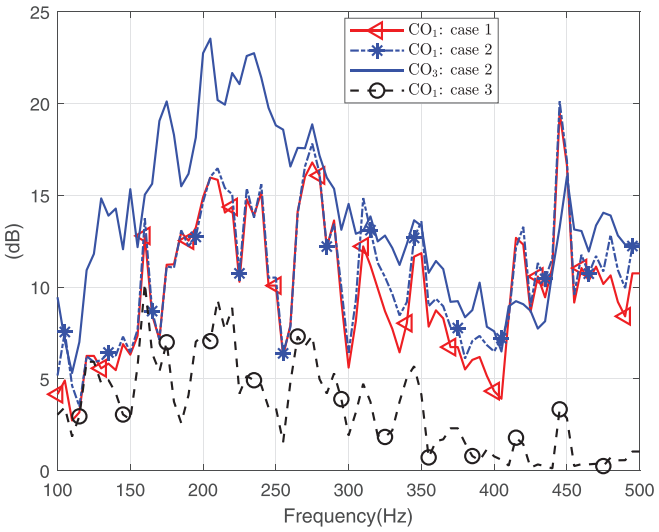

FIG. 9. (Color online) Contribution of $\mathcal{E}_{T1}$ and $\mathcal{E}_{T3}$ in different cases in the experiment.

more than the secondary sources number [Eq. (4)], the signals in the system null space (blue solid curve) have a significant contribution in the energy of the residual error, which is comparable with the contribution of coherence between error signals and reference signals (blue star curve).

V. CONCLUSIONS

In this work, we proposed a method that statistically analyzes the maximum NR performance for a multichannel ANC system. This is a powerful tool to theoretically analyze the fundamental limitation of the NR performance and investigate the contributions of each component in the energy of residual signals (1) component based on coherence between reference signals and error signals, (2) component based on the filter, and (3) component based on the noise signals in the system null space. The experimental results show that using the proposed method, we can estimate the maximum NR performance for any given ANC system. In future work, one can (1) incorporate the effect of acoustic feedback from the secondary sources to the reference sensors to the performance evaluation and (2) investigate the NR performance over a large continuous region.

ACKNOWLEDGMENTS

This research was funded partially by ARC Discovery Project Grant No. DP180102375.

APPENDIX A: PROOF OF THEOREM 1

Proof. Using the definition $S_{\hat{\nu}_r\hat{\nu}_r} = E\{\hat{\nu}_r\hat{\nu}_r^*\}$, the first term of Eq. (16) can be written as

$$E\{\hat{\boldsymbol{\nu}}^H\hat{\boldsymbol{\nu}}\} = \sum_{r=1}^{R} S_{\hat{\nu}_r\hat{\nu}_r} + \sum_{r=R+1}^{Q} S_{\hat{\nu}_r\hat{\nu}_r}. \tag{A1}$$

Since $\boldsymbol{\Sigma}$ is a rectangular diagonal matrix with R nonzero diagonal elements σ_r, $r = 1, \ldots, R$, the second term of Eq. (16) can be written as

$$\begin{aligned} E\{\hat{\boldsymbol{\nu}}^H\boldsymbol{\Sigma}\hat{\boldsymbol{W}}\boldsymbol{c}\} &= E\left\{\sum_{r=1}^{R}\sum_{z=1}^{Z}\hat{\nu}_r^*\sigma_r\hat{w}_{rz}c_z\right\} \\ &= \sum_{r=1}^{R}\sigma_r\sum_{z=1}^{Z}\hat{w}_{rz}E\{\hat{\nu}_r^*c_z\} \qquad \text{(A2)} \\ &= \sum_{r=1}^{R}\sigma_r\hat{\boldsymbol{w}}_r\boldsymbol{S}_{\hat{\nu}_r\boldsymbol{c}}^H, \qquad \text{(A3)} \end{aligned}$$

where $\hat{w}_{rz}$ is the (r, z) element of $\hat{\boldsymbol{W}}$, $\hat{\boldsymbol{w}}_r \triangleq [\hat{w}_{r1}, \ldots, \hat{w}_{rZ}]$, and the $1 \times Z$ correlation vector $\boldsymbol{S}_{\hat{\nu}_r\boldsymbol{c}} = E\{\hat{\nu}_r\boldsymbol{c}^H\}$.

Similarly, the third term in Eq. (16) can be written as

$$E\{\boldsymbol{c}^H\hat{\boldsymbol{W}}^H\boldsymbol{\Sigma}^H\hat{\boldsymbol{\nu}}\} = \sum_{r=1}^{R}\sigma_r^*\boldsymbol{S}_{\hat{\nu}_r\boldsymbol{c}}\hat{\boldsymbol{w}}_r^H. \tag{A4}$$

The fourth term in Eq. (16) can be expressed as

$$\begin{aligned} E\{\boldsymbol{c}^H\hat{\boldsymbol{W}}^H\boldsymbol{\Sigma}^H\boldsymbol{\Sigma}\hat{\boldsymbol{W}}\boldsymbol{c}\} &= E\left\{\sum_{r=1}^{R}\sum_{z=1}^{Z}\sum_{z'=1}^{Z}c_z^*c_{z'}\hat{w}_{rz}^*\hat{w}_{rz'}\sigma_r^*\sigma_r\right\} \\ &= \sum_{r=1}^{R}\sum_{z=1}^{Z}\sum_{z'=1}^{Z}|\sigma_r|^2\hat{w}_{rz}^*\hat{w}_{rz'}E\{c_z^*c_{z'}\} \\ &= \sum_{r=1}^{R}|\sigma_r|^2\sum_{z=1}^{Z}\hat{w}_{rz}^*\lambda_z\hat{w}_{rz} \\ &= \sum_{r=1}^{R}|\sigma_r|^2\hat{\boldsymbol{w}}_r\hat{\boldsymbol{\Lambda}}\hat{\boldsymbol{w}}_r^H, \qquad \text{(A5)} \end{aligned}$$

where $\hat{\boldsymbol{\Lambda}}$ is a $Z \times Z$ diagonal matrix whose diagonal elements are the nonzero diagonal elements of $\boldsymbol{\Lambda}$.

By substituting Eqs. (A1), (A3), (A4), and (A5) into Eq. (16), we obtain

$$\begin{aligned} \mathcal{E}_T = \sum_{r=1}^{R}\Big(&S_{\hat{\nu}_r\hat{\nu}_r} + \sigma_r\hat{\boldsymbol{w}}_r\boldsymbol{S}_{\hat{\nu}_r\boldsymbol{c}}^H + \sigma_r^*\boldsymbol{S}_{\hat{\nu}_r\boldsymbol{c}}\hat{\boldsymbol{w}}_r^H \\ &+ |\sigma_r|^2\hat{\boldsymbol{w}}_r\hat{\boldsymbol{\Lambda}}\hat{\boldsymbol{w}}_r^H\Big) + \sum_{r=R+1}^{Q}S_{\hat{\nu}_r\hat{\nu}_r}. \qquad \text{(A6)} \end{aligned}$$

Using the identity for completing squares for vectors, we further simplify Eq. (A6) as

$$\begin{aligned} \mathcal{E}_T = &\sum_{r=1}^{R}\left(S_{\hat{\nu}_r\hat{\nu}_r} - \boldsymbol{S}_{\hat{\nu}_r\boldsymbol{c}}\boldsymbol{\Lambda}^{-1}\boldsymbol{S}_{\hat{\nu}_r\boldsymbol{c}}^H\right) \\ &+ \sum_{r=1}^{R}\left(|\sigma_r|^2\left(\hat{\boldsymbol{w}}_r + \frac{\boldsymbol{S}_{\hat{\nu}_r\boldsymbol{c}}}{\sigma_r}\hat{\boldsymbol{\Lambda}}^{-1}\right)\right. \\ &\left.\times\hat{\boldsymbol{\Lambda}}\left(\hat{\boldsymbol{w}}_r + \frac{\boldsymbol{S}_{\hat{\nu}_r\boldsymbol{c}}}{\sigma_r}\hat{\boldsymbol{\Lambda}}^{-1}\right)^H\right) + \sum_{r=R+1}^{Q}S_{\hat{\nu}_r\hat{\nu}_r}. \qquad \text{(A7)} \end{aligned}$$

Equation (A7) can be rearranged in the form of Eq. (19) in Theorem 1. □

https://doi.org/10.1121/10.0001938

APPENDIX B: ALTERNATIVE PROOF OF THE OPTIMAL FILTER

Since $\boldsymbol{W}$ is a complex matrix and $\boldsymbol{W} = \Re(\boldsymbol{W}) + i\Im(\boldsymbol{W})$, the differentiation of Eq. (6) can be written as[20]

$$\frac{\partial \mathcal{E}_T}{\partial \boldsymbol{W}^*} = \frac{1}{2}\left(\frac{\partial \mathcal{E}_T}{\partial \Re(\boldsymbol{W})} + i\frac{\partial \mathcal{E}_T}{\partial \Im(\boldsymbol{W})}\right), \tag{B1}$$

where $\Re\{\cdot\}$ and $\Im\{\cdot\}$ denote the real part and imaginary part of a complex number, vector, or matrix, respectively.

The derivative of the real part can be expanded as

$$\begin{aligned}
\frac{\partial \mathcal{E}_T}{\partial \Re(\boldsymbol{W})} &= \frac{\partial\left[E(\boldsymbol{v}^H\boldsymbol{v})\right]}{\partial \Re(\boldsymbol{W})} + \frac{\partial\left[E(\boldsymbol{v}^H\boldsymbol{G}\boldsymbol{W}\boldsymbol{x})\right]}{\partial \Re(\boldsymbol{W})} + \frac{\partial\left[E(\boldsymbol{x}^H\boldsymbol{W}^H\boldsymbol{G}^H\boldsymbol{v})\right]}{\partial \Re(\boldsymbol{W})} + \frac{\partial\left[E(\boldsymbol{x}^H\boldsymbol{W}^H\boldsymbol{G}^H\boldsymbol{G}\boldsymbol{W}\boldsymbol{x})\right]}{\partial \Re(\boldsymbol{W})} \\
&= 0 + \frac{\partial\left[E(\boldsymbol{v}^H\boldsymbol{G}\Re(\boldsymbol{W})\boldsymbol{x})\right]}{\partial \Re(\boldsymbol{W})} + \frac{\partial\left[E(\boldsymbol{x}^H\Re(\boldsymbol{W})^H\boldsymbol{G}^H\boldsymbol{v})\right]}{\partial \Re(\boldsymbol{W})} + \cdots + \frac{\partial\left[E(\boldsymbol{x}^H(\Re(\boldsymbol{W}) + i\Im(\boldsymbol{W}))^H\boldsymbol{G}^H\boldsymbol{G}(\Re(\boldsymbol{W}) + i\Im(\boldsymbol{W}))\boldsymbol{x})\right]}{\partial \Re(\boldsymbol{W})} \\
&= E\{\boldsymbol{G}^T\boldsymbol{v}^*\boldsymbol{x}^T + \boldsymbol{G}^H\boldsymbol{v}\boldsymbol{x}^H + (\boldsymbol{G}^H\boldsymbol{G})^T\Re(\boldsymbol{W})\boldsymbol{x}^*\boldsymbol{x}^T + (\boldsymbol{G}^H\boldsymbol{G})\Re(\boldsymbol{W})\boldsymbol{x}\boldsymbol{x}^H\} + \cdots \\
&\quad + i\left\{\frac{\partial\left[E(\boldsymbol{x}^H\Re(\boldsymbol{W})^H(\boldsymbol{G}^H\boldsymbol{G})\Im(\boldsymbol{W})\boldsymbol{x})\right]}{\partial \Re(\boldsymbol{W})} + \frac{\partial\left[E(\boldsymbol{x}^H\Im(\boldsymbol{W})^H\boldsymbol{G}^H\boldsymbol{G}\Re(\boldsymbol{W})\boldsymbol{x})\right]}{\partial \Re(\boldsymbol{W})}\right\} \\
&= E\{\boldsymbol{G}^T\boldsymbol{v}^*\boldsymbol{x}^T + \boldsymbol{G}^H\boldsymbol{v}\boldsymbol{x}^H + (\boldsymbol{G}^H\boldsymbol{G})^T\Re(\boldsymbol{W})\boldsymbol{x}^*\boldsymbol{x}^T + \boldsymbol{G}^H\boldsymbol{G}\Re(\boldsymbol{W})\boldsymbol{x}\boldsymbol{x}^H + \cdots + i(\boldsymbol{G}^H\boldsymbol{G}\Im(\boldsymbol{W})\boldsymbol{x}\boldsymbol{x}^H - (\boldsymbol{G}^H\boldsymbol{G})^T\Im(\boldsymbol{W})^*\boldsymbol{x}^*\boldsymbol{x}^T)\}.
\end{aligned} \tag{B2}$$

Similar to Eq. (B2), the derivative of the imaginary part can be represented by

$$\begin{aligned}
\frac{\partial \mathcal{E}_T}{\partial \Im(\boldsymbol{W})} &= E\{i(\boldsymbol{G}^T\boldsymbol{v}^*\boldsymbol{x}^T - \boldsymbol{G}^H\boldsymbol{v}\boldsymbol{x}^H + \boldsymbol{G}^T\boldsymbol{G}^*\Re(\boldsymbol{W})\boldsymbol{x}^*\boldsymbol{x}^T \\
&\quad - \boldsymbol{G}^H\boldsymbol{G}\Re(\boldsymbol{W})\boldsymbol{x}\boldsymbol{x}^H) + \cdots \\
&\quad + \boldsymbol{G}^H\boldsymbol{G}\Im(\boldsymbol{W})\boldsymbol{x}\boldsymbol{x}^H + \boldsymbol{G}^T(\boldsymbol{G}^H)^T\Im(\boldsymbol{W})\boldsymbol{x}^*\boldsymbol{x}^T\}.
\end{aligned} \tag{B3}$$

Substitute Eqs. (B2) and (B3) into Eq. (B1) and the differentiation can be represented by

$$\begin{aligned}
\frac{\partial \mathcal{E}_T}{\partial \boldsymbol{W}^*} &= \frac{1}{2}E\{2\boldsymbol{G}^H\boldsymbol{v}\boldsymbol{x}^H + 2\boldsymbol{G}^H\mathrm{GWx}\boldsymbol{x}^H\} \\
&= E\{\boldsymbol{G}^H\boldsymbol{v}\boldsymbol{x}^H + \boldsymbol{G}^H\mathrm{GWx}\boldsymbol{x}^H\} \\
&= \boldsymbol{G}^H\boldsymbol{S}_{\boldsymbol{v}\boldsymbol{x}} + \boldsymbol{G}^H\boldsymbol{G}\boldsymbol{W}\boldsymbol{S}_{\boldsymbol{x}\boldsymbol{x}}.
\end{aligned} \tag{B4}$$

By setting

$$\frac{\partial \mathcal{E}_T}{\partial \boldsymbol{W}^*} = 0, \tag{B5}$$

we can obtain the optimal filter, which can be solved from

$$\boldsymbol{G}^H\boldsymbol{S}_{\boldsymbol{v}\boldsymbol{x}} + \boldsymbol{G}^H\boldsymbol{G}\boldsymbol{W}^o\boldsymbol{S}_{\boldsymbol{x}\boldsymbol{x}} = 0. \tag{B6}$$

Then, we represent each variable in the transformed domain. Substitute Eqs. (7), (11), (17), and (18) into Eq. (B6), then

$$\begin{aligned}
&(\boldsymbol{A}\boldsymbol{\Sigma}\boldsymbol{B}^H)^H E\{\boldsymbol{A}\boldsymbol{v}'(\boldsymbol{U}\boldsymbol{c})^H\} + (\boldsymbol{A}\boldsymbol{\Sigma}\boldsymbol{B}^H)^H(\boldsymbol{A}\boldsymbol{\Sigma}\boldsymbol{B}^H) \\
&\quad \times \boldsymbol{B}\hat{\boldsymbol{W}}^o\boldsymbol{U}^H E\{\boldsymbol{U}\boldsymbol{c}\boldsymbol{c}^H\boldsymbol{U}^H\} = 0, \\
&\boldsymbol{B}\boldsymbol{\Sigma}^H\boldsymbol{A}^H\boldsymbol{A}\boldsymbol{S}_{\boldsymbol{v}'\boldsymbol{c}}\boldsymbol{U}^H + \boldsymbol{B}\boldsymbol{\Sigma}^H\boldsymbol{A}^H\boldsymbol{A}\boldsymbol{\Sigma}\boldsymbol{B}^H\boldsymbol{B}\hat{\boldsymbol{W}}^o \\
&\quad \times \boldsymbol{U}^H\boldsymbol{U}E\{\boldsymbol{c}\boldsymbol{c}^H\}\boldsymbol{U}^H = 0, \\
&\boldsymbol{B}\boldsymbol{\Sigma}^H\boldsymbol{S}_{\boldsymbol{v}'\boldsymbol{c}}\boldsymbol{U}^H + \boldsymbol{B}\boldsymbol{\Sigma}^H\boldsymbol{\Sigma}\hat{\boldsymbol{W}}^o E\{\boldsymbol{c}\boldsymbol{c}^H\}\boldsymbol{U}^H = 0.
\end{aligned} \tag{B7}$$

As $\boldsymbol{B}$ is a unitary matrix, left multiply $\boldsymbol{B}^H$ for both sides and further simplify the result, and we can get

$$\boldsymbol{\Sigma}^H\boldsymbol{S}_{\boldsymbol{v}'\boldsymbol{c}}\boldsymbol{U}^H + \boldsymbol{\Sigma}^H\boldsymbol{\Sigma}\hat{\boldsymbol{W}}^o E\{\boldsymbol{c}\boldsymbol{c}^H\}\boldsymbol{U}^H = 0. \tag{B8}$$

As $\boldsymbol{U}$ is a unitary matrix, right multiply $\boldsymbol{U}$ for both sides and further simplify the result, and we can get

$$\boldsymbol{\Sigma}^H\boldsymbol{S}_{\boldsymbol{v}'\boldsymbol{c}} + \boldsymbol{\Sigma}^H\boldsymbol{\Sigma}\hat{\boldsymbol{W}}^o E\{\boldsymbol{c}\boldsymbol{c}^H\} = 0. \tag{B9}$$

Substitute Eq. (15) into Eq. (B9), and we can simplify Eq. (B9) as

$$\boldsymbol{\Sigma}^H\boldsymbol{S}_{\boldsymbol{v}'\boldsymbol{c}} + \boldsymbol{\Sigma}^H\boldsymbol{\Sigma}\hat{\boldsymbol{W}}^o\hat{\boldsymbol{\Lambda}} = 0. \tag{B10}$$

We write Eq. (B10) into element-wise calculation and simplify the result,

$$\sigma_r^* S_{\nu'_r c_z} + \hat{w}^o_{rz}|\sigma_r|^2\lambda_z = 0, \quad \forall r \in [1,R], \ \forall z \in [1,Z]. \tag{B11}$$

Therefore,

$$\hat{w}_{rz}^{o} = -\frac{S_{\nu_r c_z}}{\sigma_r \hat{\lambda}_z}, \quad \forall r \in [1, R], \ \forall z \in [1, Z]. \tag{B12}$$

Equation (B12) is equivalent to Eq. (22), which completes the proof.

[1]J. Cheer and S. J. Elliott, "Multichannel control systems for the attenuation of interior road noise in vehicles," Mech. Syst. Signal Process. **60-61**, 753–769 (2015).

[2]K. Iwai, S. Hase, and Y. Kajikawa, "Multichannel feedforward active noise control system with optimal reference microphone selector based on time difference of arrival," Appl. Sci. **8**, 2291 (2018).

[3]Y. Xiao, "A new efficient narrowband active noise control system and its performance analysis," IEEE Trans. Audio, Speech, Language Process. **19**(7), 1865–1874 (2011).

[4]J. Guo, F. Yang, and J. Yang, "Convergence analysis of the conventional filtered-*x* affine projection algorithm for active noise control," Signal Process. **170**, 107437 (2019).

[5]D. P. Das, D. J. Moreau, and B. S. Cazzolato, "A computationally efficient frequency-domain filtered-X LMS algorithm for virtual microphone," Mech. Syst. Signal Process. **37**(1-2), 440–454 (2013).

[6]N. K. Rout, D. P. Das, and G. Panda, "Computationally efficient algorithm for high sampling-frequency operation of active noise control," Mech. Syst. Signal Process. **56-57**, 302–319 (2015).

[7]A. A. Milani, I. M. S. Panahi, and P. C. Loizou, "A new delayless subband adaptive filtering algorithm for active noise control systems," IEEE Trans. Audio, Speech, Lang. Proc. **17**(5), 1038–1045 (2009).

[8]P. A. C. Lopes, "Active noise control algorithms with reduced channel count and their stability analysis," Signal Process. **88**(4), 811–821 (2008).

[9]L. Zhang, J. Tao, and X. Qiu, "Performance analysis of decentralized multi-channel feedback systems for active noise control in free space," Appl. Acoust. **74**(1), 181–188 (2013).

[10]J. Zhang, T. D. Abhayapala, P. N. Samarasinghe, W. Zhang, and S. Jiang, "Multichannel active noise control for spatially sparse noise fields," J. Acoust. Soc. Am. **140**(6), EL510–EL516 (2016).

[11]H. Chen, P. Samarasinghe, T. D. Abhayapala, and W. Zhang, "Spatial noise cancellation inside cars: Performance analysis and experimental results," in *2015 IEEE Workshop on Applications of Signal Processing to Audio and Acoustics (WASPAA)*, pp. 1–5.

[12]I.-H. Yang, J.-E. Jeong, U.-C. Jeong, J.-S. Kim, and J.-E. Oh, "Improvement of noise reduction performance for a high-speed elevator using modified active noise control," Appl. Acoust. **79**, 58–68 (2014).

[13]H. Chen, J. Zhang, P. N. Samarasinghe, and T. D. Abhayapala, "Evaluation of spatial active noise cancellation performance using spherical harmonic analysis," in *2016 IEEE International Workshop on Acoustic Signal Enhancement (IWAENC)*, pp. 1–5.

[14]M. De Diego and A. Gonzalez, "Performance evaluation of multichannel adaptive algorithms for local active noise control," J. Sound Vib. **244**(4), 615–634 (2001).

[15]M. Buerger, T. Abhayapala, C. Hofmann, H. Chen, and W. Kellermann, "The spatial coherence of noise fields evoked by continuous source distributions," J. Acoust. Soc. Am. **142**(5), 3025–3034 (2017).

[16]S. M. Kuo and D. Morgan, *Active Noise Control Systems: Algorithms and DSP Implementations* (Wiley, New York, 1996).

[17]J. Bitzer, K. U. Simmer, and K. Kammeyer, "Multichannel noise reduction—Algorithms and theoretical limits," in *9th European Signal Processing Conference (EUSIPCO)* (1998), pp. 1–4.

[18]S. Spors and H. Buchner, "Efficient massive multichannel active noise control using wave-domain adaptive filtering," in *3rd International Symposium on Communications, Control and Signal Processing (ISCCSP)* IEEE (2008), pp. 1480–1485.

[19]T. Kosaka, S. J. Elliott, and C. C. Boucher, "A novel frequency domain filtered-*x* LMS algorithm for active noise reduction," in *IEEE International Conference on Acoustics, Speech, and Signal Processing* (1997), Vol. 1, pp. 403–406.

[20]D. H. Brandwood, "A complex gradient operator and its application in adaptive array theory," IEE Proc., Part H: Microwaves, Opt. Antennas **130**(1), 11–16 (1983).